Comprehensive Characterization of Biochars Produced from Three Major Crop Straws of China

Siye Wei,[a,b] Mengbo Zhu,[a,b] Jianzhong Song,[a,*] and Ping'an Peng [a]

Biochars produced from rice straw, corn straw, and wheat straw under different pyrolysis temperatures were comprehensively characterized. The results indicated that the yields of the biochars decreased for all three biochar types with the increase in pyrolysis temperature from 250 °C to 600 °C. In addition, the carbon contents of the biochars increased, and the polar acidic functional groups decreased with the increase of the pyrolysis temperature. The hemicellulose and cellulose components likely decomposed at approximately 300 °C, and more condensed and ordered aromatic carbon structures were formed in the biochars with the increase in pyrolysis temperature. The results also indicated that these three types of biochars showed many similarities in elemental composition and structure. However, some differences were also observed. This work provides important baseline information for the production of biochars from crop residues with desired properties for environmental applications.

*Contact information: a: State Key Laboratory of Organic Geochemistry, Guangzhou Institute of Geochemistry, Chinese Academy of Sciences, Guangzhou 510640, P.R. China; b: Graduate School of Chinese Academy of Sciences, Beijing 100049, P.R. China; *Corresponding author: songjzh@gig.ac.cn*

INTRODUCTION

As one of the largest agricultural countries in the world, China is rich in crop straw resources, accounting for approximately 17% of global production (Bi *et al*. 2010). Rice straw (RS), corn straw (CS), and wheat straw (WS) accounted for 78% of the total output of crop straws from 1995 to 2004 in China, with an annual production of 239, 137, and 116 million tons, respectively (Liu *et al.* 2008). Open burning is typically used to efficiently and cheaply remove the crop straw residue after harvest; approximately 23% of crop straw biomass was burned in the field annually over the last few decades in China (Cao *et al.* 2008). However, the open burning of crop residues in the field not only wastes a large amount of potential biomass resources, but also releases a large amount of environmental pollutants. These pollutants include polycyclic aromatic hydrocarbons, nitrogen oxides, and greenhouse gases (CO_2), which pose a serious threat to air quality, human health, and global climate change (Woolf *et al.* 2010). Therefore, there are large incentives to find beneficial uses of crop residues that would help to alleviate agricultural residue management problems.

Returning crop straw to the soil or utilizing the straw as biomass resources for industrial applications or as biomass energy would be more reasonable than directly burning crop residues in the field (Liu *et al.* 2008). However, some difficulties are still faced by the farmers in China. Firstly, the cost of equipment is too high for the farmers; Secondly, the agricultural industrialization and production in many places of China are inadequate, which makes it difficult to recycle the crop straw sustainably; Finally, the shortage of specialist staff makes it difficult to carry out and management the reclamation.

In recent decades, the thermo-chemical conversion (*i.e.*, pyrolysis) of biomass into biochars under oxygen-free or oxygen-limited conditions has been proposed as a promising alternative technology to treat crop straws (Lehmann 2007; Woolf *et al.* 2010). The process has many benefits such as significantly reducing the volume and weight of these solid wastes in a short period of time after harvest.

Both heat and gases released from the pyrolytic conversation of biomass could be used as valuable renewable bioenergy. Carbon-rich biochar can be also a good soil amendment and mix with manures or fertilizers due to its potential benefits in the quality of agricultural soils (Lehmann *et al.* 2003; Yuan *et al.* 2011). In addition, as an ideal adsorbing material, biochar could be used as a tool for adsorbing and capturing environmental contaminants and reducing their bioavailability in water and soils (Lehmann 2007). Moreover, biochar is a recalcitrant form of carbon that can exist for hundreds to thousands of years in soil. This means that it has high carbon storage potential (Lehmann *et al.* 2003) and has been recommended as a possible tool to sequester CO_2, thereby aiding in reducing global warming (Mohanty *et al.* 2013).

The application potential of specific biochar types greatly depends on their inherent physicochemical properties. The properties of biochar are first affected by the nature of the original materials. For instance, biochar produced from crop straw generally exhibits a higher yield, ash content, and pH than the wood-based biochars (Wang *et al.* 2013). The pyrolysis conditions, in particular, the pyrolysis temperature, are another key factor influencing the biochar properties. Biochar produced at a high pyrolysis temperature is characterized by a large surface area and aromatic carbon content, which may increase the adsorption capacity as well as its recalcitrant character (Lehmann 2007). Although the characteristics of biochars derived from crop residues have been reported in some studies, most have only focused on the physical and chemical properties of one or two crop residue biochars. There has been little consideration of the comprehensive characterization of biochars produced from different crop straws along a wide range of pyrolysis temperatures. Nonetheless, if biochars are to be created with desired properties for specific purposes and for promoting agricultural residue management production, the development of effective production procedures is crucial.

In this study, rice, wheat, and corn straws were used to investigate the pyrolysis of crop straws due to the large quantity of these three crop straws and their low utilization rates. In addition, these crop residues are generally considered good feedstock materials for making biochars due to their environmental and financial viability (Cao and Harris 2010).

The aim of this study was to comprehensively investigate the chemical composition and structure of the different types of biochars formed at a wide range of pyrolysis temperatures. Biochars from these three major crop residues were first produced under various pyrolysis temperatures of 250 °C, 300 °C, 350 °C, 400 °C, 500 °C, and 600 °C. These biochars were then characterized using an elemental analyzer, Boehm titration, thermogravimetric analysis (TGA), and Raman spectrometry. The results are essential for understanding the potential applications of biochars for environmental and agronomic management and for evaluating their suitability for carbon sequestration.

EXPERIMENTAL

Materials

In this study, biochars were produced from the pyrolysis of crop straws under oxygen-limited conditions. Three typical agricultural residues, including RS, CS, and WS, were chosen because they account for major components of crop straws produced in China and are also important agricultural residues worldwide. The RS was collected in the Zhengguo town of the Guangdong Province of south China, and the CS and WS were collected in a suburb of Xinyang city in the Henan Province in a mid-eastern region of China. The crop straws were first washed with tap water and dried for 24 h at 80 °C. Then the samples were wrapped two-fold in aluminum foil to minimize oxidation, placed in a muffle furnace (Shanghai Jia Zhan Instrumentation Equipment Ltd., Shanghai, China) (Hall *et al.* 2008), and pyrolysed at a heating rate of 5 °C /min at peak temperatures of 250 °C, 300 °C, 350 °C, 400 °C, 500 °C, and 600 °C for 2 h, respectively. The weight of the biochar was recorded, and the biochar yield was calculated by mass balance. The biochar samples were hereafter referred to as RS X00 (rice straw), CS X00 (corn straw), and WS X00 (wheat straw), with X representing the final pyrolysis temperature (250 °C, 300 °C, 350 °C, 400 °C, 500 °C, and 600 °C, respectively).

Methods

The elemental compositions (C/H/N) of the three types of crop-derived biochars were measured using an elemental analyzer (Elementar Vario El Cube, Hanau, Germany), and the ash content of samples was determined by heating the sample in an open crucible in a muffle furnace at 750 °C for 6 h. The weight of sample was taken after cooling in a desiccator for 24 h. The oxygen content was calculated by mass balance: O% = 100% - (C + H + N + ash)%. The pH values and acidic functional groups of the biochars were determined using the Boehm titration method (Chun *et al*. 2004; Mukherjee *et al.* 2011). The thermal analysis (thermogravimetric/TG) of biochar samples was performed on a STA490 PC thermal analyzer (Netzsch-Gerätebau GmbH, Netzsch, Switzerland) coupled with a differential thermal analyzer (DTA). The experiments were performed from 30 °C to 1000 °C at a heating rate of 10 °C/min. Nitrogen was used as the carrier gas with a flow rate of 100 mL/min. Then, Raman spectroscopy was investigated on a micro-laser Raman spectrometer (HORIBA-JY Xplora, Paris, France) fitted with a 532 nm solid laser device. The microscope observation was set to a 50x objective lens to focus the laser beam on the microcosmic surface of the biochars. The exposure time was 10 s. The Raman spectra were recorded from 100 cm^{-1} to 3200 cm^{-1} on five different spots of each biochar sample.

RESULTS AND DISCUSSION

Yield and Ash Content

The changes in the yield and ash content of biochars of RS, CS, and WS produced at different pyrolysis temperatures are shown in Fig. 1. The three types of crop-derived biochars shared similar trends, in that the biochar yields all decreased with the increased pyrolysis temperature, due to the greater thermal decomposition of organic fractions in the crop straws. As indicated in Fig. 1, the yields of biochar were decreased noticeably from 59.9±0.8 wt.% to 31.7±0.5 wt.% for RS, from 72.0±1.5 wt.% to 27.7±1.0 wt.% for

CS, and from 70.1 ± 1.6 wt.% to 30.4 ± 1.3 wt.% for WS, respectively, as the pyrolysis temperature increased from 250 °C to 600 °C. The results observed in this study were similar to other studies of biomass-based biochars (Keiluweit *et al.* 2010). These declines were mainly due to the release of moisture and volatile organic compounds in the biochars, as well as the decomposition of hemicelluloses, cellulose, and lignin (Table 1) (Demirbas 2004; Al-Wabel *et al.* 2013) with increased pyrolysis temperature. Moreover, a large decrease in yield occurred before 300 °C, which was similar to the observation of Keiluweit *et al*. (2010). This decrease was likely due to the decomposition and destruction of organic compounds, such as cellulose and hemicellulose in the biomass (Keiluweit *et al*. 2010). In addition, the slow decrease of the yields from 300 °C to 600 °C could likely be attributed to the complete degradation of relative thermal resistant organic matter at temperatures above 300 °C.
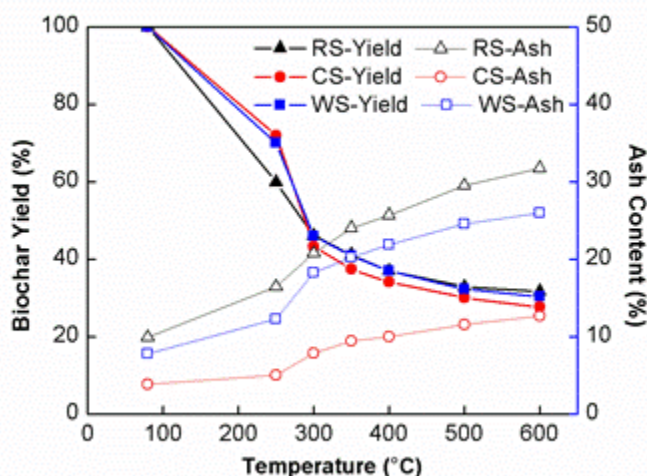
Fig. 1. The yield and ash content of biochars produced from RS, CS, and WS at different temperatures

Table 1. The Proximate and Lignocellulosic Contents of RS, CS, and WS

Samples	Proximate analysis (wt %)				Lignocellulosic content (wt %)		
	Moisture	Volatiles matter	Fixed Carbon	Ash	Cellulose	Hemicellulose	Lignin
RS	6.94±0.22	63.4±0.2	19.7±0.5	9.93±0.21	34.9±0.7	23.4±0.5	23.5±0.3
CS	11.6±0.6	65.2±0.5	19.3±0.3	3.88±0.12	35.6±2.0	20.2±1.5	22.9±0.4
WS	11.7±0.4	60.6±0.5	19.8±0.7	7.81±0.31	32.6±1.6	22.2±1.4	24.1±0.2

By contrast, the ash content of the three types of crop straw biochars all increased noticeably as the temperature was increased from 250 °C to 600 °C (Fig. 1). For example, the percentage of ash content of RS increased from 9.93 ± 0.21 wt.% for feedstock to 16.4 ± 0.8 wt.%, 20.8 ± 1.5 wt.%, 24.1 ± 1.2 wt.%, 25.7 ± 0.7 wt.%, 29.5 ± 0.9 wt.%, and 31.8 ± 1.2 wt.%, for biochars formed at 250 °C, 300 °C, 350 °C, 400 °C, 500 °C, and 600 °C, respectively. These results were similar to those produced from other agricultural wastes, such as bagasse, rice husk, and cow biosolid (Shinogi and Kanri 2003), and should have resulted from the progressive condensation of minerals and destructive volatilization of

lignocelluloses matter during the pyrolytic process (Tsai *et al*. 2012). It is noted that the ash content of the three types of crop straw-derived biochars was different, ranging in the order of RS (16.4 wt.% to 31.8 wt.%) > WS (12.3 wt.% to 26.0 wt.%) > CS (5.02 wt.% to 12.7 wt.%).

Elemental Composition

The elemental composition (C/H/N/O) of the studied biochars (including raw materials) is shown in Table 2. The C content in the biochar tended to increase and the H and O contents tended to decrease with increased temperature. The increase in the carbon content with increased temperature could have been due to the increased degree of carbonization, while the losses of O and H at high temperatures may have been attributed to the cleavage and cracking of weaker bonds within the biochar structure (Demirbas 2004).

Table 2. Elemental Composition, Atomic Ratio, Yield, and Ash Content of Biochars Produced from RS, CS, and WS

Sample	Elemental Compositions						Atomic Ratios			Yield (%)
	C%	H%	O%	N%	Ash%	Sum%	O/C	H/C	(N+O)/C	
RS	39.2±0.2	5.48±0.90	44.8±0.3	0.51±0.01	9.93±0.21	99.9±0.2	0.86±0.02	1.68±0.06	0.87±0.01	100.0±0.0
RS250	50.8±1.2	5.40±0.29	26.9±0.2	0.45±0.01	16.4±0.8	101.0±1.9	0.40±0.01	1.28±0.10	0.41±0.02	59.9±0.8
RS300	59.1±0.2	5.15±0.08	14.4±0.8	0.56±0.01	20.8±1.5	101.0±1.6	0.18±0.01	1.05±0.02	0.19±0.00	46.1±1.2
RS350	58.9±0.2	4.50±0.01	12.0±0.3	0.58±0.05	24.1±1.2	100.5±0.9	0.15±0.01	0.92±0.00	0.16±0.01	41.2±0.7
RS400	61.7±0.1	3.31±0.00	8.6±0.1	0.66±0.04	25.7±0.7	101.1±0.6	0.10±0.02	0.64±0.03	0.11±0.01	37.0±0.6
RS500	61.6±0.4	3.19±0.07	5.06±0.08	0.68±0.04	29.5±0.9	101.3±1.4	0.06±0.00	0.62±0.01	0.07±0.01	32.9±0.3
RS600	62.9±0.4	2.84±0.09	1.87±0.01	0.60±0.06	31.8±1.2	100.0±1.7	0.02±0.01	0.54±0.01	0.03±0.01	31.7±0.5
CS	43.1±0.3	6.72±0.06	45.7±0.3	0.62±0.03	3.88±0.12	101.3±1.2	0.80±0.02	1.87±0.11	0.81±0.02	100.0±0.0
CS250	53.4±0.1	6.22±0.10	35.1±0.7	0.26±0.01	5.02±0.14	100.6±1.5	0.49±0.02	1.40±0.02	0.50±0.02	72.0±1.5
CS300	68.9±0.2	5.61±0.07	17.1±0.2	0.59±0.04	7.86±0.09	100.1±0.8	0.19±0.01	0.98±0.01	0.19±0.01	43.3±0.9
CS350	69.5±0.6	4.89±0.15	15.6±0.6	0.61±0.04	9.46±0.17	100.1±1.9	0.17±0.02	0.84±0.03	0.18±0.02	37.5±1.1
CS400	74.4±0.4	3.75±0.01	10.9±0.1	0.69±0.03	10.0±0.6	99.7±0.8	0.11±0.01	0.60±0.03	0.12±0.01	34.2±0.7
CS500	78.1±0.2	3.66±0.06	5.84±0.5	0.80±0.08	11.6±0.5	100.0±0.1	0.06±0.01	0.56±0.01	0.06±0.00	30.0±1.4
CS600	82.0±0.1	3.06±0.23	1.50±0.41	0.82±0.05	12.7±1.5	100.1±1.3	0.01±0.00	0.45±0.03	0.02±0.00	27.7±1.0
WS	40.6±0.1	6.66±0.03	44.1±0.3	0.88±0.16	7.81±0.31	100.2±0.1	0.81±0.05	1.97±0.05	0.83±0.05	100.0±0.0
WS250	49.6±0.1	6.05±0.17	31.4±0.2	0.67±0.04	12.3±1.3	101.3±1.6	0.47±0.09	1.46±0.04	0.49±0.02	70.1±1.6
WS300	60.8±0.3	5.36±0.11	14.5±0.1	1.12±0.01	18.3±0.9	100.1±0.9	0.18±0.03	1.06±0.02	0.19±0.01	46.0±2.5
WS350	61.3±0.1	4.59±0.06	12.8±0.2	1.06±0.17	20.2±0.6	101.0±0.5	0.16±0.03	0.90±0.01	0.17±0.03	40.9±1.3
WS400	62.8±0.3	3.30±0.02	10.9±0.5	1.07±0.10	21.9±0.9	101.0±1.2	0.13±0.02	0.63±0.00	0.14±0.02	37.0±0.7
WS500	66.4±0.2	3.36±0.04	4.43±0.9	1.19±0.06	24.6±0.6	101.4±1.6	0.05±0.01	0.61±0.01	0.07±0.01	32.3±0.4
WS600	67.7±0.1	2.60±0.17	2.59±0.6	1.08±0.05	26.0±1.1	100.8±1.2	0.03±0.00	0.46±0.03	0.04±0.01	30.4±1.3

The calculated atomic ratios of the biochars derived from H/C, O/C, and (O + N)/C of RS, CS, and WS are shown in Table 2. The atomic ratio of H/C could be a good parameter to describe the degree of carbonization of the biochar samples (Chun *et al.* 2004), while the O/C and (O + N)/C atomic ratios represented the polar functional groups of biochars. These results indicated that the raw crop straw samples possessed the highest atomic ratio values, and these ratios exhibited a declining trend with increased temperature. For example, the H/C atomic ratio decreased from 1.68-1.97 of raw crop straws to 0.45-0.54 of biochars at 600 °C, and their O/C atomic ratio decreased from 0.80-0.86 to 0.01-0.03, respectively. These data indicated the increased aromaticity, maturation degree, and the continuous reduction of the polar functional groups of biochars in relation to increased pyrolysis temperature.

The H/C and O/C atomic ratios of crop straws and their biochars produced at different temperatures are also shown in a van Krevelen diagram (Fig. 2). Both the H/C and O/C atomic ratios decreased with increased temperatures. Briefly, the H/C *versus* O/C exhibited a moderately decreasing slope below 300 °C, while the decreasing slope became sharper between 300 °C and 600 °C. The slow decrease in H/C and O/C at low temperatures (< 300 °C) could have been due to the initial dehydration and the dehydrogenation and demethylation of organic matter, such as hemicelluloses, cellulose, and lignin materials in the biochars. Likewise, the rapid decreases in H/C and O/C at high temperatures (more than 350 °C) may have been the result of the decarboxylation and demethylation of organic matter in the biochars at high pyrolysis temperatures (Demirbas 2004; Al-Wabel *et al.* 2013). These results also indicated that the chemical compostion and structure of biochars were noticeably changed when the pyrolysis temperature was more than 350 °C.
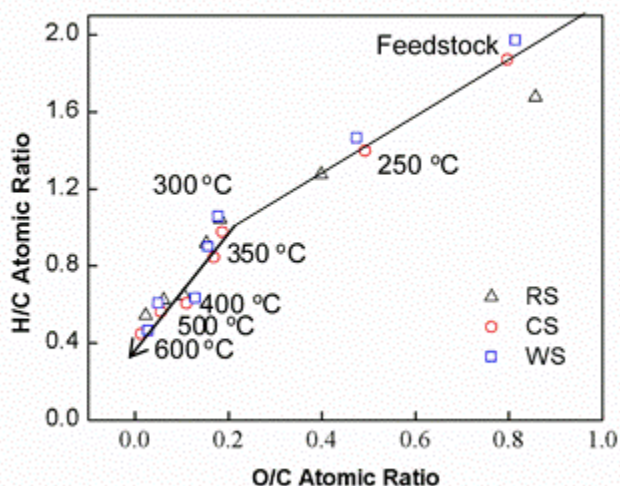

Fig. 2. Van Krevelen diagram of the three types of biochars and original crop straws

pH and Boehm Titration

As shown in Table 3, the pH values of RS-, CS-, and WS-derived biochars all tended to increase with increased pyrolysis temperatures. For example, the pH value increased from 6.97 ± 0.12 to 7.81 ± 0.63, 8.43 ± 0.21, 9.13 ± 0.23, 10.39 ± 0.13, and 10.56 ± 0.15 for RS biochar formed at 250 °C, 300 °C, 350 °C, 400 °C, 500 °C, and 600 °C, respectively. This was in agreement with the results reported in previous studies (Yuan *et al.* 2011), which indicated that higher pyrolysis temperatures led to a higher pH in biochars.

The raw material samples usually had a relatively neutral pH, while the pyrolysis-derived biochars fell in the range of weakly basic to alkaline, dependent on the pyrolysis temperature. The biochars formed at higher pyrolysis temperatures had higher pH values. This was mainly due to the degradation of the acidic functional groups, such as carboxyl and phenolic hydroxyl groups, as well as the formation of alkalis as the charring temperature increased (Yuan *et al.* 2011; Wang *et al.* 2013). Among the three types of biochars, no large differences in pH values were observed.

Table 3. The pH and Boehm Titration Results of Biochars Produced from RS, CS, and WS

Sample	Boehm Titration (mmol/g)			Carboxyl/Acidic	pH
	Carboxyl	Phenolic	Acidic		
RS250	0.33±0.05	0.79±0.14	1.32±0.12	0.25±0.03	6.97±0.12
RS300	0.29±0.03	0.76±0.11	1.23±0.15	0.24±0.05	7.81±0.63
RS350	0.32±0.05	0.44±0.07	0.77±0.10	0.42±0.04	8.43±0.21
RS400	0.28±0.02	0.30±0.03	0.62±0.06	0.45±0.07	9.13±0.23
RS500	0.28±0.01	0.08±0.01	0.43±0.03	0.65±0.09	10.39±0.13
RS600	0.11±0.02	0.33±0.02	0.47±0.05	0.23±0.03	10.56±0.15
CS250	0.35±0.05	0.83±0.12	1.32±0.13	0.27±0.02	7.92±0.12
CS300	0.72±0.11	1.46±0.25	2.22±0.23	0.32±0.04	7.93±0.22
CS350	0.65±0.07	1.28±0.10	1.93±0.12	0.34±0.03	8.83±0.56
CS400	0.52±0.08	0.79±0.08	1.31±0.18	0.40±0.06	9.93±0.24
CS500	0.36±0.02	0.20±0.01	0.56±0.06	0.64±0.10	10.02±0.32
CS600	0.30±0.02	0.22±0.06	0.52±0.07	0.58±0.08	9.95±0.27
WS250	0.59±0.09	0.96±0.11	1.55±0.21	0.38±0.01	6.78±0.12
WS300	0.44±0.06	0.87±0.16	1.31±0.17	0.34±0.02	7.67±0.32
WS350	0.34±0.08	0.49±0.04	0.83±0.10	0.41±0.06	8.39±0.54
WS400	0.32±0.01	0.39±0.07	0.71±0.09	0.45±0.07	9.58±0.32
WS500	0.26±0.04	0.12±0.02	0.38±0.03	0.68±0.06	10.31±0.21
WS600	0.22±0.03	0.24±0.03	0.46±0.06	0.48±0.10	10.45±0.15

The functional groups on the surface of the biochars were measured by titration, according to Boehm (Mukherjee *et al.* 2011). Generally, the amount of total surface acidic groups of biochars decreased as the pyrolysis temperature increased. Table 3 shows that the relatively higher total surface acidity generally existed in the low-pyrolysis temperature-derived biochars from the RS and WS, while a relatively lower total surface acidity was detected in the high pyrolysis temperature-derived biochars. However, for biochars derived from CS, the amount of total acidic functional groups varied. First they increased (from 1.32±0.13 mmol/g to 2.22±0.23 mmol/g) with the rise in temperature from 250 °C to 300 °C, and then they gradually decreased (from 2.22±0.23 mmol/g to 0.52±0.07 mmol/g) when the temperature increased from 300 °C to 600 °C. Both the carboxyl and phenolic groups showed a similar decreasing trend for the CS-derived biochars.

Notably, the ratio of the carboxyl groups to total acidic functional groups of the three types of biochars all showed a steady increasing trend from 250 °C to 500 °C. For example, the ratio of carboxyl/acidic for CS biochar increased from 0.27±0.02 at 250 °C to 0.32±0.04, 0.34±0.03, 0.40±0.06, and 0.64±0.10 at 300 °C, 350 °C, 400 °C, and 500 °C, respectively. This result may have been due to the decomposition of weak acidic groups, such as the phenolic and lectonic groups, with increased pyrolysis of the biomass materials (Luo *et al.* 2015). However, this ratio decreased when the pyrolysis temperature was increased to 600 °C, which was possibly due to the loss of carboxyl groups in the biochar at the high temperature.

Thermogravimetric Analysis

As shown in Fig. 3, the thermal decomposition of the three crop straws and their corresponding biochars occurred in the total range of experimental temperatures. Different types of biochars produced at the same pyrolysis temperature exhibited a similar trend in weight loss over the range of pyrolysis temperatures.

In general, the thermal decomposition of these biochar samples in the study could be divided into three stages according to the thermogravimetric and differential thermogravimetric (TG-DTG) analysis curves. The first stage (below 200 °C) was a minor weight loss at a maximum temperature of approximately 80 °C, customarily due to the release of moisture volatilization and some organic constituents from the raw materials. In the second stage (between 200 °C to 600 °C), a major decomposition occurred, associated with the progressive degradation of organic compounds, such as hemicellulose, cellulose, and lignin (Yang *et al*. 2007; Cao and Harris 2010). The hemicellulose degraded easily at 220 °C to 315 °C; the cellulose decomposed at a higher temperature (from 315 °C to 400 °C), and the composition of lignin covered a wide range of heating temperatures (from 150 °C to 900 °C) (Yang *et al.* 2007). Finally, in the last stage (above 600 °C), a slight weight loss was observed, which was attributed to the decomposition of the thermal resistant chemical structures, such as lignin, charred materials, *etc*. In addition, it was reported that the crystallization of mineral components and conformation of highly ordered aromatic structures in biochars might increase in this high pyrolysis temperature stage (Al-Wabel *et al.* 2013).

Figure 3 shows that the mass losses of biochars formed at different pyrolysis temperatures were clearly different. The mass loss of biochars formed at lower temperatures was higher than that of biochars formed at higher temperatures. As an example, the total weight loss of RS biochars at the final temperature of 1000 °C decreased from 50.7 wt.% for RS250 to 35.0 wt.%, 23.7 wt.%, 19.9 wt.%, 14.6 wt.%, and 11.9 wt.% for RS300, RS350, RS400, RS500, and RS600, respectively. These results indicated that more stable forms of condensed carbon structures in the biochars formed at the high temperatures.

As shown in Fig. 3, the degradation behavior of the three types of biochars was clearly different from each other. For example, the total weight loss of RS, CS, and WS at the final temperature of 1000 °C was 67.4%, 70.0%, and 68.2%, respectively, which indicated the different thermal degradation characteristics of those crop materials at that high of a temperature. The diverse thermal behavior could have been due to the differences in the inherent structures and the chemical nature of the three crop straw materials (Table 1).
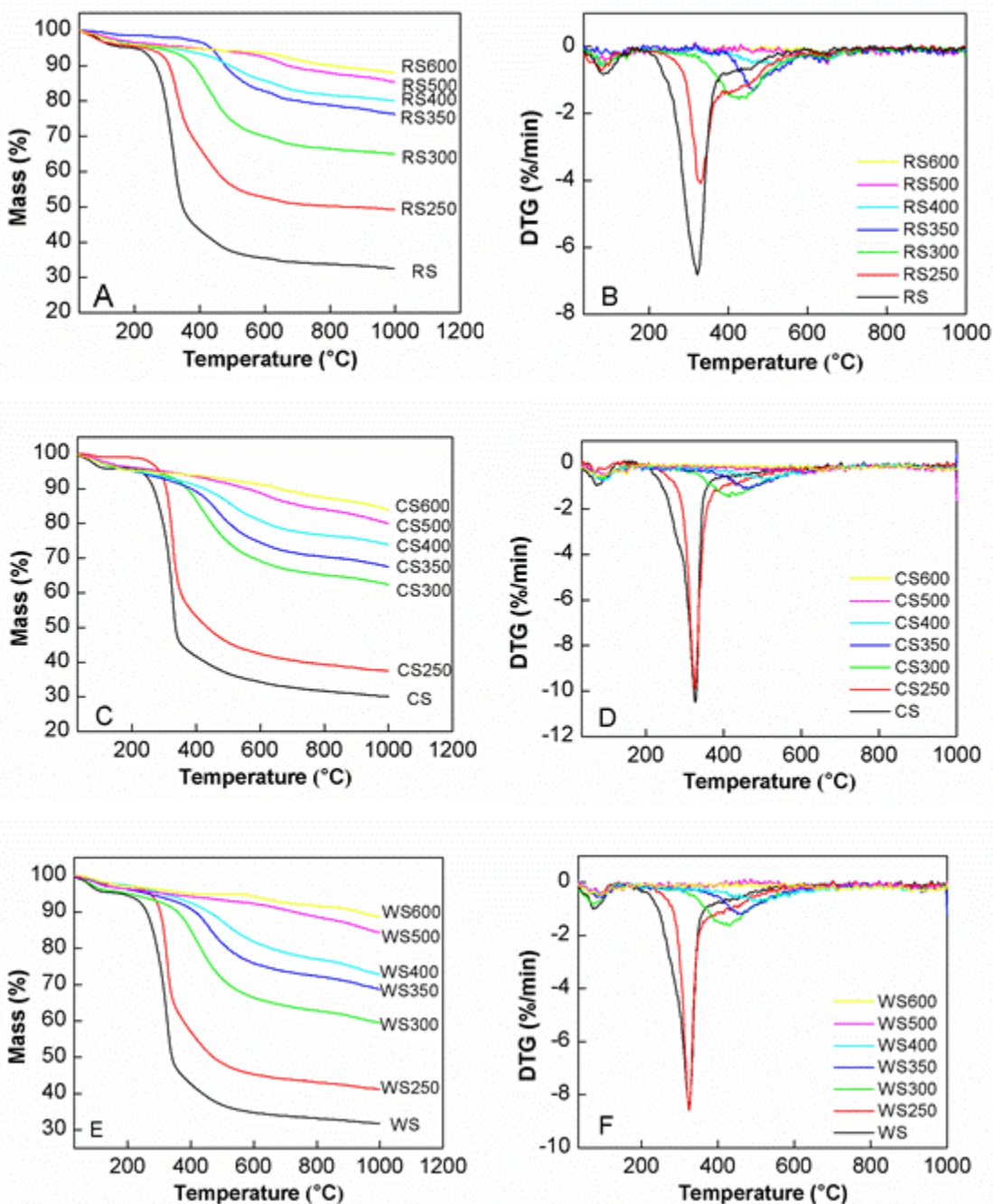
Fig. 3. TG and DTG curves of the three types of biochars and original crop straws: (A, B) RS, (C, D) CS, and (E, F) WS

The TG and DTG curves of RS250, CS250, and WS250 exhibited some similar thermal degradation behavior to their feedstocks. The main weight loss of these samples took place at 200 °C to 400 °C, where the maximum pyrolysis temperature at 322.2 °C, 326.8 °C, and 325.3 °C corresponded to the maximum pyrolysis rate of 6.83 wt.%/min, 10.5 wt.%/min, and 8.42 wt.%/min for RS, CS, and WS, respectively. The maximum pyrolysis temperature at 332.2 °C, 325.8 °C, and 324.8 °C corresponded to the maximum

pyrolysis rate of 4.09 wt.%/min, 9.90 wt.%/min, and 8.58 wt.%/min for RS250, CS250, and WS250, respectively, and those were all thought to be related to the degradation of cellulose. These results suggested that the cellulose components in raw crop straws may survive in the biochars formed at 250 °C.

The TG curves of biochars produced at 300 °C to 400 °C were not greatly changed, excluding the percentage of mass loss when compared to that of raw materials and biochars produced at 250 °C. However, the DTG curves became much broader between 300 °C and 400 °C (Fig. 3), and the higher pyrolysis temperature-derived biochars exhibited a higher DTG peak temperature and lower mass loss rate. For example, the maximum pyrolysis temperatures were 406.2 °C, 414.7 °C, and 461.8 °C for the CS biochar formed at 300 °C, 350 °C, and 400 °C, respectively, which were noticeably higher than the 325.8 °C for the CS biochar formed at 250 °C. Meanwhile, the corresponding maximum pyrolysis rates of CS biochar decreased from 9.90 wt.%/min for CS250 to 1.47 wt.%/min, 1.11 wt.%/min, and 0.70 wt.%/min for CS300, CS350, and CS400, respectively.

Furthermore, the TG-DTG results clearly showed that for biochars produced at 500 °C and 600 °C, the mass loss ratio hardly changed with the increased pyrolysis temperature and the overall decomposition processes accounted for the remaining weight loss less than 16.1 wt.%. in the CS biochar sample weight at 600 °C. These results suggested that the biochars produced at higher temperatures (500 °C and 600 °C) mainly consisted of high thermal resistant, condensate structures.

Raman Analysis

Raman spectroscopy is an effective method to illuminate the crystalline and amorphous carbon structures present in biochar materials, especially for biochars produced at high pyrolysis temperatures (Mohanty *et al.* 2013). The Raman shift around 1350 cm^{-1} is associated with the in-plane vibrations of disordered graphite rings (D-band), while the Raman peak near 1580 cm^{-1} mainly comes from the vibrations of double bonds and sp^2 bonded in crystalline graphite (G-band) (Paris *et al.* 2005; Mohanty *et al.* 2013). In this sense, the properties of D-bands and G-bands are very useful parameters to understand the microstructure features of the carbon in biochars. The ratio of the integrated intensities of the D and G peaks (I_D/I_G), has often been used to evaluate the average crystallite thickness, which was often inversely proportional to the crystallite size (La) of graphite materials (Paris *et al.* 2005).

Typical Raman spectra of the three types of biochars from 100 cm^{-1} to 3200 cm^{-1} are shown in Fig. 4. No clearly identifiable Raman spectra were observed for the feedstocks and biochars produced at 250 °C due to strong fluorescence (Paris *et al.* 2005). As the pyrolysis temperatures were raised to 300 °C, the influence of the fluorescence was diminished and could be ignored. Two broad Raman peaks near 1350 cm^{-1} (D-bands) and 1580 cm^{-1} (G-bands) were identified in the Raman spectra, which signified the formation of aromatic carbons and aromatic graphene with increased temperature. Both the D-bands and G-bands of biochar samples showed an increasing trend in intensity and sharpness with increased pyrolysis temperature. However, there were no remarkable differences in the D-band and G-band positions among the biochars produced at different temperatures for the three types of biochars. The D-band positions showed a gradual shift to lower wave numbers (*e.g*., from 1357.14 cm^{-1} to 1344.63 cm^{-1} for RS), while the G-band positions hardly changed as the pyrolysis temperatures increased from 300 °C to 600 °C. As a result, the inter-peak intervals of the D-band and G-band positions (*d*(G-D)) increased from 227.24 cm^{-1} to 243.41 cm^{-1}, 213.73 cm^{-1} to 251.58 cm^{-1}, and 214.57 cm^{-1} to 245.65 cm^{-1}

for RS-, CS-, and WS-derived biochars from 300 °C to 600 °C, respectively (Fig. 4). The changes in the d (G-D) showed that the aromaticity and maturity of biochars increased with the increased pyrolysis temperatures.
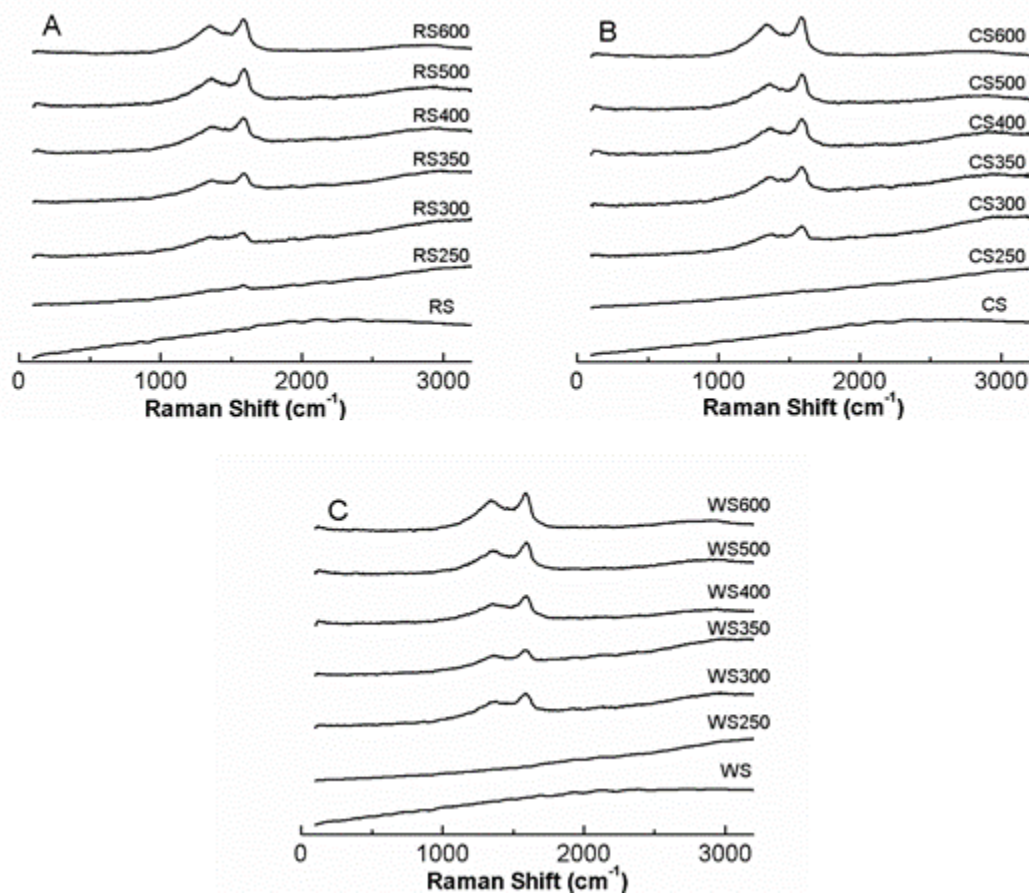
Fig. 4. Raman spectra of the three types of biochars and original crop straws: (A) RS, (B) CS, and (C) WS

The I_D/I_G ratios (peak areas) in the three types of biochars derived from crop straws increased from 2.26 to 2.41, 2.13 to 2.60, and 2.08 to 2.38 for RS-, CS-, and WS-derived biochars from 300 °C to 600 °C, respectively. Similar results were also reported in the study of Yamauchi and Kurimoto (2003), who found that the I_D/I_G ratio of biochars obtained from wood and bark samples clearly increased from 500 °C to 800 °C. That indicated that the concentration of aromatic rings containing six or more fused benzene rings increased with the increase in pyrolysis temperature (Nanda *et al*. 2014). The increases in the aromatic degree and resistance in biochars produced at higher temperatures created the potential for the long-term use of biochars in the carbon sequestration in soil to mitigate climate change.

Comparison of Biochars Produced from the Three Major Crop Straws

The biochars formed from the three major crop straws were compared and characterized in this study. The results indicated some similarities and differences among these biochar samples.

Similarities

The changes in chemical characteristics of biochars including organic component and mineral component in relation to increasing pyrolysis temperatures were very similar for the three types of crop straws. For example, the three types of biochars exhibited similar decreasing trends in yield as the pyrolysis temperature increased from 250 °C to 600 °C. In addition, the ash contents of biochars from the three crop straws also increased with increased pyrolysis temperature, which indicated the accumulation of inorganic materials (Tsai *et al*. 2012). These may be due to the three feedstocks contain similar proximate and lignocellulosic components (Table 1).

Many similarities were further revealed by detailed analysis of the organic component of biochars from different crop straws. According to the results of elemental analysis, the contents of C in the biochar all tended to increase along with the contents of H and O. Also, the atomic ratios of H/C, O/C, and (O + N)/C tended to decrease with increased temperature. These observations suggested that similar pyrolysis reactions occurred for the three crop straws. During the pyrolysis process, the degree of carbonization gradually increased and the O and H content and some polar functional groups were continuously reduced with increased temperature. Moreover, the pH values and functional groups showed similar change trends with increased pyrolysis temperatures. For example, the pH values of the biochars all increased and the amount of total surface acidic groups of biochars all decreased as the pyrolysis temperature increased. More similarities were also identified by the TGA and Raman analyses. For example, the intensity of the peaks in the D-band and G-band, d(G-D), and the I_D/I_G ratios of biochars derived from the three crop straws increased as the pyrolysis temperature increased, suggesting that the aromaticity and maturity of biochars increased with increased pyrolysis temperatures.

Differences

Although the biochars formed at the same temperature were very similar, there were some differences in the chemical composition and characteristics among the three types of biochars. At first, some differences were found by comparing the organic component among biochars from different crop straws. Initially, the C content of CS-derived biochars was slightly higher than that in both the RS- and WS-derived biochars ($p < 0.05$), while the N content in the WS-derived biochars was higher than the other two types of biochars ($p < 0.05$). The thermal degradation behaviors (such as final total weight loss, maximum pyrolysis temperature, and maximum pyrolysis rate of the three types of biochars) were also different from each other due to the chemical diversity of the feedstock materials. For example, the total weight loss of CS at the final temperature of 1000 °C was 70.0 wt.%, which was considerably more than the 67.4 wt.% and 68.2 wt.% for RS and WS, respectively. These differences can be explained by relative low ash content of CS. The maximum pyrolysis temperatures of RS, CS, and WS were at 322.2 °C, 326.8 °C, and 325.3 °C, respectively, with corresponding maximum pyrolysis rates of 6.83 wt.%/min, 10.5 wt.%/min, and 8.42 wt.%/min, respectively.

Moreover, the inorganic minerals (ash) content of the three types of biochars formed at the same temperature was different, ranging in the order of RS > WS > CS. The relatively higher ash content in the biochars of RS and WS may have been the result of more material components present in the original RS and WS.

CONCLUSIONS

1. The results of this study showed that both the type of crop straw materials and pyrolysis temperature greatly influences the physicochemical and structural characteristics of the biochars, and the former one seems more important, which in turn affects their potential applications.

2. The three type of biochars produced at low pyrolysis temperatures (< 300 °C) all had relatively higher yields. They also still retained some polar functional groups, such as hydroxyl, carboxyl, carbonyl, *etc.*, which might have positive effects on soil quality and increase the sorptive capacity of biochar for ionic solutes. Therefore they are suitable for agricultural use.

3. The degree of aromatization of biochar obtained from all crop straws began to accelerate with the increasing pyrolysis temperature. Above 500 °C, and the liable functional groups tended to be removed completely, leaving the dominated aromatic carbon with low H/C and O/C ratios. Therefore, for the purpose of amending acid soil or long-term sequestration in soil, it is preferable to maintain a relatively higher pyrolysis temperature (≥ 500 °C).

ACKNOWLEDGEMENTS

REFERENCES CITED

Al-Wabel, M. I., Al-Omran, A., El-Naggar, A. H., Nadeem, M., and Usman, A. R. A. (2013). "Pyrolysis temperature induced changes in characteristics and chemical composition of biochar produced from conocarpus wastes," *Bioresource Technol.* 131, 374-379. DOI: 10.1016/j.biortech.2012.12.165

Bi, Y. Y., Wang, Y. J., and Gao, C. Y. (2010). "Straw resource quantity and its regional distribution in China," *J. Agr. Mech. Res.* (03), 1-7. DOI: 10.3969/j.issn.1003-188X.2010.03.001

Cao, G. L., Zhang, X. Y., Wang, Y. Q., and Zheng, F. C. (2008). "Estimation of emission from field burning of crop straw in China," *Chinese Sci. Bull.* (53), 784-790. DOI: 10.1007/s11434-008-0145-4

Cao, X. D., and Harris, W. (2010). "Properties of dairy-manure-derived biochar pertinent to its potential use in remediation," *Bioresource Technol.* 101(14), 5222-5228. DOI: 10.1016/j.biortech.2010.02.052

Chun, Y., Sheng, G. Y., Chiou, C. T., and Xing, B. S. (2004). "Compositions and sorptive properties of crop residue-derived chars," *Environ. Sci. Technol.* 38(17), 4649-4655. DOI: 10.1021/es035034w

Demirbas, A. (2004). "Effects of temperature and particle size on bio-char yield from pyrolysis of agricultural residues," *J. Anal. Appl. Pyrol.* 72(2), 243-248. DOI:

10.1016/j.jaap.2004.07.003

Hall, G., Woodborne, S., Scholes, M. (2008). "Stable carbon isotope ratios from archaeological charcoal as palaeoenvironmental indicators," *Chem. Geol.* 247(3-4), 384-400. DOI:10.1016/j.chemgeo.2007.11.001

Keiluweit, M., Nico, P. S., Johnson, M. G., and Kleber, M. (2010). "Dynamic molecular structure of plant biomass-derived black carbon (biochar)," *Environ. Sci. Technol.* 44(4), 1247-1253. DOI: 10.1021/Es9031419

Lehmann, J. (2007). "A handful of carbon," *Nature* 447(7141), 143-144. DOI: 10.1038/447143a

Lehmann, J., Da Silva, J. P., Steiner, C., Nehls, T., Zech, W., and Glaser, B. (2003). "Nutrient availability and leaching in an archaeological Anthrosol and a Ferralsol of the Central Amazon basin: Fertilizer, manure, and charcoal amendments," *Plant Soil* 249(2), 343-357. DOI: 10.1023/A:1022833116184

Liu, H., Jiang, G. M., Zhuang, H. Y., and Wang, K. J. (2008). "Distribution, utilization structure, and potential of biomass resources in rural China: With special references of crop residues," *Renew. Sust. Energ. Rev.* 12(5), 1402-1418. DOI: 10.1016/j.rser.2007.01.011

Luo, L., Xu, C., Chen, Z., and Zhang, S. Z. (2015). "Properties of biomass-derived biochars: Combined effects of operating conditions and biomass types," *Bioresource Technol.* 192, 83-89. DOI: 10.1016/j.biortech.2015.05.054

Mohanty, P., Nanda, S., Pant, K. K., Naik, S., Kozinski, J. A., and Dalai, A. K. (2013). "Evaluation of the physiochemical development of biochars obtained from pyrolysis of wheat straw, timothy grass, and pinewood: Effects of heating rate," *J. Anal. Appl. Pyrol.* 104, 485-493. DOI: 10.1016/j.jaap.2013.05.022

Mukherjee, A., Zimmerman, A. R., and Harris, W. (2011). "Surface chemistry variations among a series of laboratory-produced biochars," *Geoderma* 163(3-4), 247-255. DOI: 10.1016/j.geoderma.2011.04.021

Nanda, S., Azargohar, R., Kozinski, J. A., and Dalai, A. K. (2014). "Characteristic studies on the pyrolysis products from hydrolyzed canadian lignocellulosic feedstocks," *Bioenerg. Res.* 7(1), 174-191. DOI: 10.1007/s12155-013-9359-7

Paris, O., Zollfrank, C., and Zickler, G. A. (2005). "Decomposition and carbonisation of wood biopolymers- a microstructural study of softwood pyrolysis," *Carbon* 43(1), 53-66. DOI: 10.1016/j.carbon.2004.08.034

Shinogi, Y., and Kanri, Y. (2003). "Pyrolysis of plant, animal, and human waste: Physical and chemical characterization of the pyrolytic products," *Bioresource Technol.* 90(3), 241-247. DOI: 10.1016/S0960-8524(03)00147-0

Tsai, W. T., Liu, S. C., Chen, H. R., Chang, Y. M., and Tsai, Y. L. (2012). "Textural and chemical properties of swine-manure-derived biochar pertinent to its potential use as a soil amendment," *Chemosphere* 89(2), 198-203. DOI: 10.1016/j.chemosphere.2012.05.085

Wang, Y., Hu, Y. T., Zhao, X., Wang, S. Q., and Xing, G. X. (2013). "Comparisons of biochar properties from wood material and crop residues at different temperatures and residence times," *Energ. Fuel.* 27(10), 5890-5899. DOI: 10.1021/ef400972z

Woolf, D., Amonette, J. E., Street-Perrott, F. A., Lehmann, J., and Joseph, S. (2010). "Sustainable biochar to mitigate global climate change," *Nat. Commun.* 1, 56. DOI: 10.1038/ncomms1053

Yamauchi, S., and Kurimoto, Y. (2003). "Raman spectroscopic study on pyrolyzed wood and bark of Japanese cedar: Temperature dependence of Raman parameters," *J. Wood*

Sci. 49(3), 235-240. DOI: 10.1007/s10086-002-0462-1

Yang, H. P., Yan, R., Chen, H. P., Lee, D. H., and Zheng, C. G. (2007). "Characteristics of hemicellulose, cellulose, and lignin pyrolysis," *Fuel* 86(12-13), 1781-1788. DOI: 10.1016/j.fuel.2006.12.013

Yuan, J. H., Xu, R. K., and Zhang, H. (2011). "The forms of alkalis in the biochar produced from crop residues at different temperatures," *Bioresource Technol.* 102(3), 3488-3497. DOI: 10.1016/j.biortech.2010.11.018